Proton-Coupled Hole Transfer in X-irradiated Doped Crystalline Cytosine·H_2O

André Krivokapić,*,† Janko N. Herak,‡ and Einar Sagstuen†

Department of Physics, University of Oslo, P.O. Box 1048 Blindern, N-0316 Oslo 3, Norway, and Faculty of Pharmacy and Biochemistry, University of Zagreb, Croatia

Received: October 9, 2007; In Final Form: February 5, 2008

Following exposure to X-irradiation at low temperatures, the main reactions taking place in single crystals of cytosine monohydrate doped with minute amounts of 2-thiocytosine are hole transfer (HT) from the electron-loss centers to the dopant and recombination of oxidation and reduction products, assumedly by electron transfer. A huge deuterium kinetic isotope effect (KIE; $>10^2-10^3$) at 100 K, together with the kinetic curves obtained and density functional theory (DFT) calculations of equilibrium energy changes, indicates that these reactions proceed through a concerted proton-coupled electron/hole transfer where the proton transfer occurs between hydrogen-bonded cytosine molecules. The temperature dependence of these reaction rates between 10 and 150 K in normal and partially deuterated samples was investigated by monitoring the growth and decay of the various radical species over time using electron paramagnetic resonance (EPR) spectroscopy. By assuming a random distribution of the hole donors and acceptors in the crystals, the data are consistent with an exponential distance-dependent rate, giving a distance decay constant (β) around 1 $Å^{-1}$ for the HT, which indicates that a long-range single-step superexchange mechanism mediates the charge transfer. The reactions undergo a transition from a slow, weakly temperature-dependent rate to an Arrhenius-type rate at 40−50 K, presumably being activated by excitation of low-frequency intermolecular vibrations that couple to the process. Below this transition temperature, the transfer probability might be dominated by temperature-independent nuclear tunneling. A similar β value in both temperature regions suggests that hopping is not activated.

1. Introduction

Proton-coupled electron transfer (PCET)[1−4] is an important mechanism in a number of chemical and biological redox reactions and may play a crucial role in radical reactions in irradiated biological molecular systems. Previous electron paramagnetic resonance (EPR) and electron nuclear double resonance (ENDOR) studies of X-irradiated crystalline DNA base derivatives have shown that the initially formed electron-addition and electron-loss radicals tend to stabilize by protonation and deprotonation reactions, respectively, with the proton transfers taking place along hydrogen bonds in the matrix.[5−8] Proton transfer (PT) is also believed to stabilize primary base-centered radicals in irradiated DNA. Following exposure to ionizing radiation, holes migrate to guanine because of its lower ionization potential, and excess electrons become trapped on cytosine and thymine, which have a high electron affinity. The reduced cytosine may become stabilized by PT from its complementary base guanine. Similarly, oxidized guanine may stabilize by transferring a proton to cytosine.[9,10] Experimental evidence is available indicating that the oxidation of guanine[11,12] and hole hopping between guanines[13] in DNA occur through PCET reactions.

Common to these systems is that the primary (de)protonated radicals are stable only at low temperatures. Upon warming, recombination and charge shift reactions become activated, in which the electron/hole transfer could be coupled with back-transfer of the protons.[14,15] The proton and the electron are transferred in different directions, distinguishing the process from the more studied cases where both the electron- and the proton-transfer take place between the same molecules. It is thus of interest to investigate the charge-transfer mechanism in more detail in a model system having these features.

In the present report, EPR spectroscopy is used to study the temperature effect and deuterium kinetic isotope effect (KIE) of hole transfer (HT) and recombination in a model system consisting of X-irradiated crystalline cytosine monohydrate (C) doped with small amounts of 2-thiocytosine (TC). TC has a lower ionization potential than C[16] and acts as a hole acceptor in this system at low temperatures.[17−19] The radicals predominantly formed at 10 K have previously been characterized by ENDOR.[18,20] These are the N1 deprotonated cytosine cation (radical *R*C), the N3 protonated cytosine anion (radical *R*A), and the N1 deprotonated thiocytosine cation (radical *R*S), as shown in Chart 1.

The radicals have all been stabilized by PT along the hydrogen bond between N1 and N3 of neighboring bases. The previous study showed an increase in radical *R*S upon thermal annealing,[17] indicating effective net HT from radical *R*C to TC. This process may be expected to be coupled with back-transfer of the proton across the N1···N3 bond. Correspondingly, PT may be necessary for recombination of these radicals.

2. Experimental Section

2.1. Crystallography and Methods. Single crystals of cytosine monohydrate and partially deuterated cytosine monohydrate crystals, with all oxygen- and nitrogen-bonded protons

* Corresponding author. Phone: +47 228 57687. Fax: +47 228 55671. E-mail: andre.krivokapic@fys.uio.no.
† University of Oslo.
‡ University of Zagreb.

10.1021/jp709855c CCC: $40.75
Published on Web 03/15/2008

CHART 1

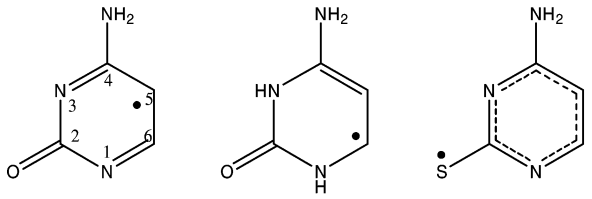

Radical RC *Radical RA* *Radical RS*

CHART 2

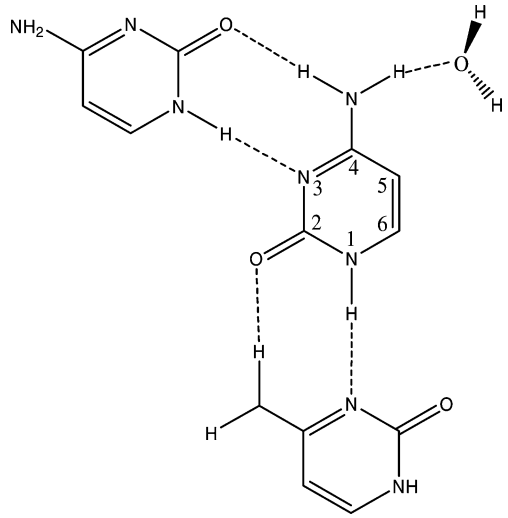

exchanged with deuterons, doped with 2-thiocytosine, were prepared as previously described.[18] A total of 20 crystals were studied. The doping level varied between 0 and 0.8 mol % and was determined by 500 MHz ^{1}H NMR spectroscopy. Because of the sulfur substituent, the chemical shift of the HC5 proton of 2-thiocytosine deviates sufficiently from that of the corresponding proton of cytosine to give a well-resolved resonance line that enables an estimation of the molar concentration of TC in the crystals, similar to what was done for other doped crystals.[21] It will be assumed that the thiocytosines are randomly distributed in the crystals, replacing the cytosine molecules while the lattice structure remains virtually unchanged.

Crystals of cytosine monohydrate are monoclinic with a space group $P2_1/c$ and with four asymmetric units in the crystal cell. The molecules are hydrogen-bonded in parallel ribbons which are linked into a three-dimensional network by hydrogen bonding through the water molecules. The amino protons are hydrogen-bonded to a water molecule and to O2 of a neighboring base. O2 is further hydrogen-bonded to two water molecules. The proton at N1 is hydrogen-bonded to N3 of a neighboring base.[22,23] Chart 2 shows the H bonding between cytosine molecules (including one water molecule).

The experimental procedures including instrumentation, X-ray diffraction, X irradiation, and X-band EPR spectroscopy were mainly as previously described.[18] EPR measurements were done with a Bruker Elexsys 560 SuperX spectrometer, with a Cr^{3+} reference mounted independently in the cavity. The measurements were done at the temperature of irradiation (10−60 K) and at elevated temperatures. The samples were X-irradiated (60kV/40mA) inside the cavity vacuum shroud for 2 h to a dose of about 19 kGy, which is below the saturation region of the dose−response relationship.[19]

DFT calculations were performed using the Gaussian03 program package.[24] The initial geometry of the cytosine monohydrate system was taken from the neutron diffraction study.[23] Geometries of reactants and products in various protonation states were optimized using the B3LYP functional and the 6-31+G(d) basis set, whereas single point calculations were performed at the optimized geometries using the 6-311+G-(2df,p) basis set. The energies were corrected for zero-point vibrations determined at the level of optimization.

2.2. Spectrum Analysis. All EPR spectra were acquired with the magnetic field aligned perpendicular to <*b*> and about 60° from <*c**>. At this position in the *ac** plane, the signal from the thiocytosine radical (*R*S) is separated maximally from the remaining resonance lines due to its higher *g* value.[25] During the spectral analysis, the necessary corrections were made for differences in sample masses and microwave power, which was kept low (0.002−0.08 mW) at all temperatures to avoid power saturation.[19] Spectra acquired at different temperatures were compared by taking into account the Boltzmann distribution of the spin population. The energy absorption is proportional to the difference in the number of spins aligned parallel and antiparallel to the magnetic field at thermal equilibrium. To first order, this population difference becomes inversely proportional to the temperature. This approximation may be applied when $h\nu$ (the resonance energy) $\ll k_BT$ (the thermal energy), which for X-band frequencies occurs at temperatures > ∼10 K.

The spectra were reconstructed by using simulated benchmark spectra of the components in a linear least-squares regression routine of MS Excel 2002, producing as fitting parameters the percentage contribution of the components and the r^2 value of the fitting. Double integration of these weighted components then gives the relative contributions from the various radicals. The simulations were made with the program KVASAT.[26,27] At low temperatures (<60 K), apparently only the radicals in Chart 1 were present. The EPR spectra of the cytosine radicals were simulated using hyperfine coupling tensors previously obtained[20] and nitrogen coupling tensors corresponding to the spin distribution proposed in that paper. For optimum fit the spectra of radicals *R*C and *R*A were simulated using a Lorentzian line-shape, which provided a significantly better fit than the Gaussian line-shape. A singlet was used to reconstruct the spectrum of radical *R*S. Figure 1 shows examples of experimental and reconstructed EPR spectra of normal and deuterated doped crystals, X-irradiated and recorded at 10 K.

According to the reconstruction, the oxidation and reduction products were generally present in about equal amounts for all of the samples at all of the investigated temperatures, and this distribution is assumed in the analysis below. When normal (H_2O) crystals were warmed to 60 K and above, a third component seemed to appear in the same spectral region as for radicals *R*C and *R*A. The spectral shape of this component was estimated by subtracting simulated spectra of *R*C and *R*A from the experimental spectra in order to eliminate the lines from these components. The resultant spectra consisted mostly of a doublet with a splitting of around 1.5 mT, a line width of about 0.3−0.4 mT, and a *g* value of approximately 2.0047. The doublet was present in both doped and undoped crystals, implying a cytosine centered radical. Apparently, it grew in at the expense of the protonated anion (*R*A), suggesting a possible conversion of this radical.

A simulated doublet was thus included in the spectrum reconstruction, which improved the fit significantly. The relative contribution of this component (in an undoped crystal) increased from a few percent at 60 K to about 20% at 150 K. It appeared to be stable at 60−85 K, whereas upon annealing to 100 K, an initial (absolute) increase was followed by a slow, steady decline. At 150 K, it decayed in the same proportion as the

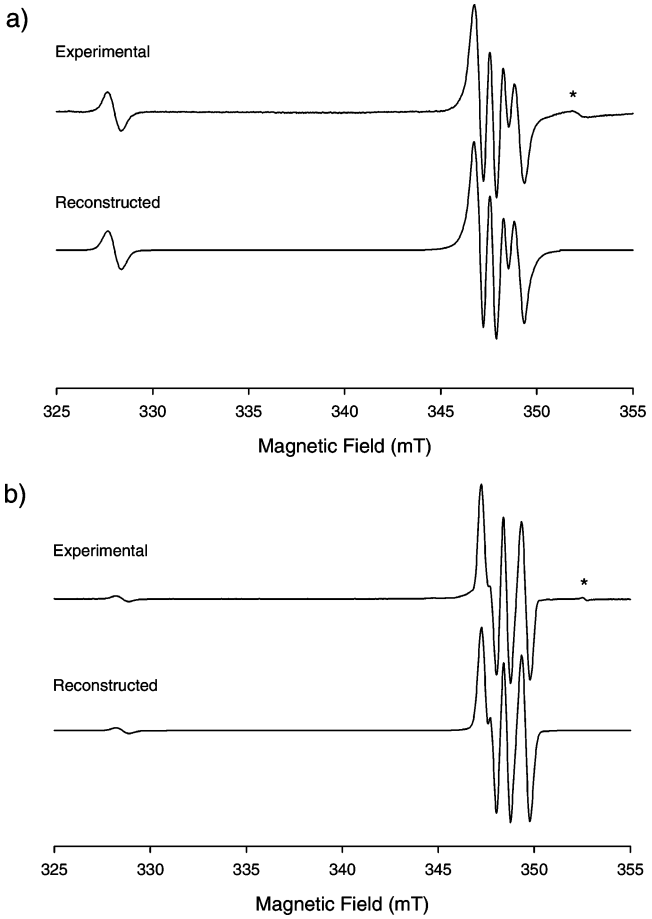

Figure 1. Experimental and reconstructed X-band EPR spectra of single crystals of cytosine monohydrate doped with 2-thiocytosine. The magnetic field is aligned perpendicular to <b> and about 60° from <c*>. (a) Spectra from a 0.3 mol % doped normal (H_2O) crystal. (b) Spectra from a partially deuterated 0.15 mol % doped crystal. The lines in the low-field region are from radical *R*S. The asterisks indicate the Cr^{3+}marker lines. The r^2 factors were >0.99.

other two cytosine radicals. For the deuterated crystals, however, no new component appeared in the spectra until temperatures of 100−110 K were reached. Unfortunately, it was not possible to determine the spectral shape of this additional component; the above-mentioned doublet appeared not to be the proper spectral shape. This suggests a key role of the exchangeable protons for its formation. It is unknown which radical the doublet represents. For all of the crystals, the r^2 value for the spectrum reconstruction decreased both with increasing temperature and with time at the higher temperatures.

3. Results

3.1. Hole Transfer. The signal intensities due to the various radicals were measured as a function of time after irradiation and as a function of time after warming to various temperatures. The main reactions taking place are growth of radical *R*S and recombination of oxidation and reduction products (mainly radicals *R*C and *R*A) and a possible conversion of radical *R*A. Figure 2 shows an example of the variation of the radical concentrations (the four components used in the reconstruction) with time in a normal doped crystal that was irradiated at 10 K and warmed to 75 K. The left part of the figure shows the concentrations relative to the total radical yield at 1 min after warming, while the right part shows the radical fractions where the sum is normalized to unity for each spectrum and plotted on a logarithmic time scale. The plots illustrate both that radical

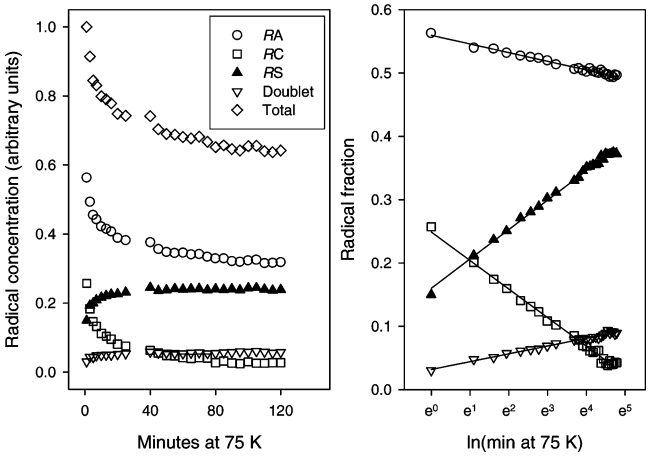

Figure 2. Concentration of the radical species in a normal crystal (doping level 0.42 mol %) irradiated at 10 K and warmed to 75 K. Left: Radical concentrations relative to the total radical yield at 1 min after warming. Right: Fractions of the different radical species where the sum is normalized to unity at the various times after warming and plotted on a logarithmic time scale to highlight the growth of radical *R*S at the expense of *R*C. The lines are linear fits to the data.

*R*S is formed at the expense of radical *R*C, which implies hole transfer (HT) from *R*C to TC, and the possible conversion of radical *R*A.

Figure 3 shows examples of the absolute growth of radical *R*S with time for two normal and one deuterated crystal at various temperatures. The samples were irradiated at approximately 10 K and stepwise warmed to the temperatures indicated. For the normal crystals, annealing to 30 K results in a small (filled symbols) or no (open symbols) increase of the rate of radical *R*S formation, while the rate increases considerably after annealing to 60 K. The markedly slower rate in the deuterated crystal indicates a coupling to proton transfer (see below). For simplicity, when determining the rate parameters in the analysis below, the reaction is referred to as HT. Radical *R*S started to decay between 100 and 150 K in normal crystals and between 140 and 170 K in deuterated crystals.

It will be assumed that the HT probability is exponentially dependent on the distance *R* between hole donor and acceptor. The transfer rate may then be expressed as[28]

$$k = k_0 \exp[-\beta(R - R_0)] \quad (1)$$

where β is the distance decay constant and R_0 is the smallest separation of donor and acceptor,[29] which, on the basis of the crystal structure for the present system, is taken to be 3 Å.[22,23] The factor k_0 includes the electronic coupling at distance R_0 and the Franck−Condon weighted density of states, where the latter are taken to be independent of donor−acceptor distance and time.[30] The extensive hydrogen-bonding network in the crystals as well as the partial base-stacking presumably gives rise to a three-dimensional electronic coupling between the bases and correspondingly a three-dimensional HT probability. Since orientation effects are unknown, the transfer probability is treated as isotropic, and the parameter values obtained are therefore orientation-averaged.

To estimate k_0 and β from the experimental data, *R* is considered to be a time-dependent tunneling radius associated with a reaction volume (sphere) around the donors within which the HT occurs. Then, in the absence of competing reactions, for a random[31,32] distribution of donors (*R*C) and acceptors (TC), where the concentration of donors is much less than the

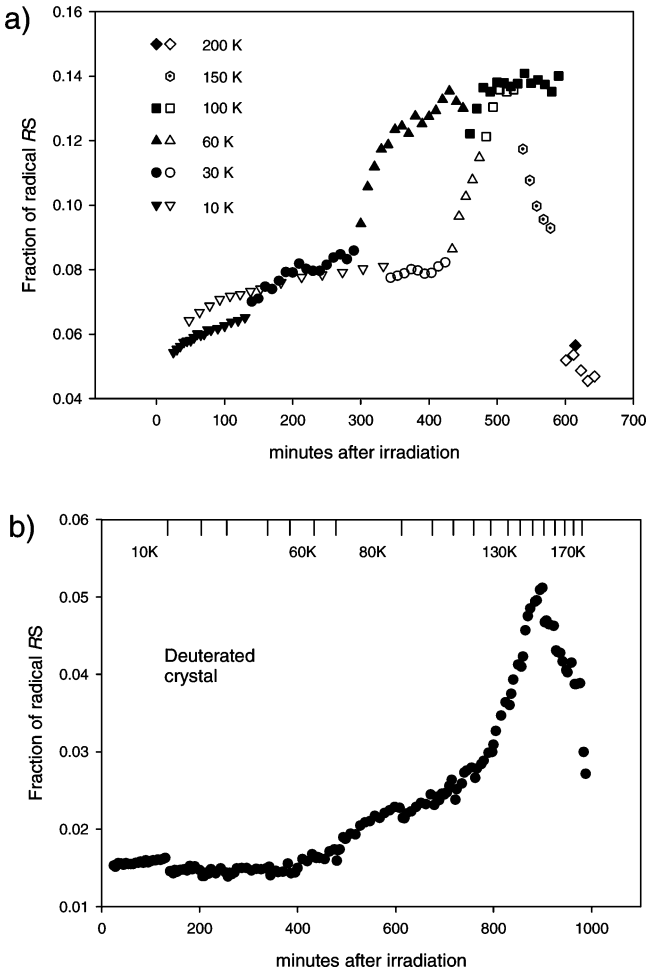

Figure 3. Absolute increase of radical *R*S with time and temperature in single crystals of cytosine (H_2O/D_2O) doped with thiocytosine. The radical fractions are given relative to the total radical yield after irradiation at 10 K. (a) A 0.29 mol % (filled symbols) and a 0.36 mol % (open symbols) doped H_2O crystal. (b) A 0.15 mol % doped deuterated crystal. The crystals were irradiated at 10 K and warmed to the temperatures indicated. The crystal in b was warmed in steps of 10 K indicated by the upper ticks at the corresponding times after irradiation. The sudden drop in concentration between some temperatures is probably due to inaccuracies of sample temperatures.

concentration of acceptors, the surviving fraction $P(t)$ of donors at time t is approximately[29,30,33]

$$P(t) = \exp\left[-\frac{4}{3}\pi c(R^3 - R_0^3)\right] \quad (2)$$

where c is the molar concentration of acceptors and is given by $c = N_A{*}d/V_M$, where N_A is Avogadro's number, d is the doping level (in mol %), and V_M is the molar volume which for crystalline cytosine H_2O is 87.25 cm^3/mol.[22] Rearrangement of eq 2 gives for R

$$R = [R_0^3 - (3/4\pi c) \ln P(t)]^{1/3} \quad (3)$$

The exponential distance dependence of the rate enables R to be expressed as[29,30,33,34]

$$R = R_0 + (1/\beta) \ln (k_0 t) \quad (4)$$

The fraction of radical *R*S is used throughout as a measure of the donor surviving fraction P because of the separate and easily measurable signal of this radical (Figure 1) and because donors may be lost to recombination, as discussed below. In the absence of recombination, the amount of *R*S that increases equals the amount of donors decreasing.

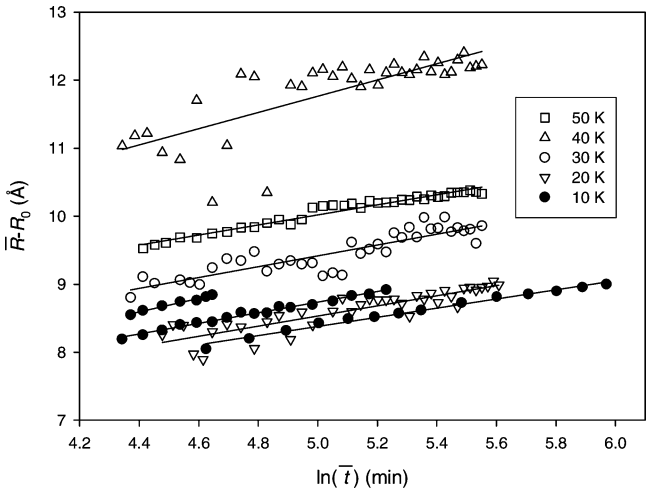

Figure 4. Tunneling distance as a function of time for HT in seven single crystals of cytosine·H_2O doped with thiocytosine, calculated by eqs 2−6. The crystals were irradiated and observed at the temperatures indicated. The lines are linear fits to the data. The rate parameters along with doping levels are given in Table 1 and were obtained as explained in the text.

It is problematic, however, to use eq 4 directly to determine the HT rate at the temperature of irradiation since the irradiation time t_{irr} (2 h) is significant as compared with the observation time. Therefore, HT occurring during irradiation needs to be taken into account as well. To surmount this complication, the simplifying assumption is made that the surviving probability of the donors is independent of the presence of other previously or subsequently formed donors, which may hold true when the radical concentration is low. Separating the donors into infinitesimal fractions corresponding to the time t' of their formation ($0 < t' < t_{irr}$) makes eq 4 applicable for each fraction individually; the transfer range for each fraction may then be expressed as $r = R_0 + (1/\beta) \ln[k_0(t + t')]$ where t is the time after irradiation (observation time). Since the system is approximately in the linear dose−response region,[19] the number of donors formed may be expressed as at_{irr}, where a is some constant. The average range for all fractions at time t is then $\bar{R} = \int_0^{t_{irr}} ra\, dt' / \int_0^{t_{irr}} a\, dt' = 1/t_{irr} \int_0^{t_{irr}} r\, dt'$. Now, if all of the donors were formed at the same instant, this average range would also be obtained at some particular time $\bar{t}$ after their formation. Expressing this average range on the form of eq 4 then gives

$$\bar{R} = R_0 + (1/\beta) \ln(k_0 \bar{t}) = 1/t_{irr} \int_0^{t_{irr}} \{R_0 + (1/\beta) \ln[k_0(t + t')]\}\, dt' \quad (5)$$

Solving for $\ln(\bar{t})$ further yields

$$\ln(\bar{t}) = \frac{t + t_{irr}}{t_{irr}} \ln(t + t_{irr}) - \frac{t}{t_{irr}} \ln t - 1 \quad (6)$$

This "average" time $\bar{t}$ is used in the left-hand side of eq 5 to determine k_0 and β for the samples at the irradiation temperature. (It follows from eq 6 that when $t \gg t_{irr}$, $\bar{t}$ asymptotically approaches $t + t_{irr}/2$.)

Figure 4 shows plots of $\bar{R} - R_0$ as a function of $\ln(\bar{t})$ obtained for normal samples irradiated and observed at 10 to 50 K. Values for k_0 and β are found from the slope of the curves ($1/\beta$) and from the interception at the ordinate (at $1/\beta \ln(k_0)$) and are given in Table 1. The results indicate no significant increase of k_0

TABLE 1: Rate Constants (k_0) and the Distance Decay Constant (β) for HT in Normal and Partially Deuterated Single Crystals of Cytosine·H_2O Doped with Thiocytosine (Uncertainties Are Based on the Data Fitting Alone)

T (K)	$\log(k_0)$ (s^{-1})	β ($Å^{-1}$)	d (mol %)	$r^{2\,d}$
		H_2O		
10[a]	0.61 ± 0.14	1.28 ± 0.04	0.29	0.992
10	1.1 ± 0.2	1.48 ± 0.05	0.36	0.988
10[b]	−0.2 ± 0.1	1.01 ± 0.06	0.32	0.972
20	0.7 ± 0.5	1.34 ± 0.12	0.34	0.987
30	0.9 ± 0.5	1.25 ± 0.11	0.34	0.991
40	0.05 ± 0.6	0.84 ± 0.13	0.34	0.983
50	1.7 ± 0.2	1.36 ± 0.05	0.79	0.982
60[a]	2.4 ± 0.3	1.15 ± 0.06	0.29	0.988
75	4.5 ± 0.7	1.3 ± 0.1	0.42	0.976
85[b]	5.4 ± 0.3	1.31 ± 0.05	0.32	0.979
100	7.7 ± 1.3	0.9 ± 0.1	0.08	0.967
		D_2O		
85[c]	−0.6 ± 0.2	1.1 ± 0.1	0.47	0.990
100	1.0 ± 0.4	1.2 ± 0.1	0.19	0.981
100	−0.4 ± 0.1	0.72 ± 0.03	0.27	0.973
130[c]	1.1 ± 0.15	0.93 ± 0.03	0.47	0.979

[a,b,c] Same crystals that have been warmed. [d] Average value for the spectrum reconstructions.

within the temperature range 10−40 K. Nor does it appear to be any systematic change in β.

Upon irradiation at 10−30 K, the total radical yield was approximately constant during the observation time, whereas upon irradiation at 40 and 50 K, a small reduction (5−10%) occurred after 2 h. To correct for the loss of donors due to recombination a correction procedure was applied for the donor surviving fraction P, as explained below.[35] Irradiation at 60 K did not lead to an observable increase of radical *R*S with time. This may be ascribed to activated recombination and a substantial higher HT rate, making the reactions occur before spectrum acquisition can take place. For the deuterated crystals, the HT rate was too low at low temperatures (<85 K) to be estimated at the time scale employed (2−3 h).

HT at higher temperatures (≥60 K) was studied by irradiating the samples at 10 K followed by warming. At these temperatures, a substantial portion of the donors is lost to recombination with radical *R*A, while the acceptor radical *R*S remains stable, so the donor surviving fraction will no longer solely reflect the HT efficiency.

One approach to correct for this loss of donors could be to compare the surviving fractions of donors in doped and undoped crystals.[33] Unfortunately, because of technical reasons, radical concentrations in different samples could not be adequately compared for correction purposes. Nevertheless, a lower limit for the surviving fraction P could be obtained. The following reactions were considered:

$$RC + TC \rightarrow C + RS(\text{hole transfer}) \quad (7a)$$

$$RC + RA \rightarrow C + C(\text{recombination}) \quad (7b)$$

Denoting the time dependent probabilities for reactions 7a and 7b by p and q, respectively, and assuming that these probabilities are mutually independent, the surviving fraction of donors, relative to the initial concentration of donors, after a period of time, will be $[RC]/[RC]|_{t=0} = (1 - p)(1 - q)$. The quantity of interest with regard to HT is $(1 - p) = P$ (the surviving fraction of donors in the absence of recombination). The higher stability of the acceptor radical *R*S gives that $(1 - q) < ([RC]+[RS])/[RC]|_{t=0}$ (where $(1 - q)$ is the donor surviving fraction in the absence of hole acceptors), and consequently that $(1 - p) > ([RC]/([RC] + [RS])$. The decay of *R*C makes this latter fraction decrease with time even though no HT to the acceptors should occur. To avoid registering erroneously an apparent HT, for each measurement i, the fraction must be determined by considering only the increase of [*R*S] relative to the preceding measurement, that is $\Delta[RS]_i = [RS]_i - [RS]_{(i-1)}$. A lower limit for P at the nth measurement is then

$$P_n > \prod_{i=1}^{n} \frac{[RC]_i}{[RC]_i + \Delta[RS]_i} = P_{\min,n} \quad (8)$$

An upper limit for P would be obtained by considering only the absolute increase of radical *R*S with time, that is, $P < (1 - [RS]/[RC]|_{t=0}) = P_{\max}$. However, not taking into account the substantial diminishing amount of donors due to recombination makes this limit unsuitable for making comparisons between different temperatures. The true value of P is probably closer to the lower limit (eq 8), which was therefore used to determine the rate parameters.

An additional problem arises when warming the crystals since upon reaching a new temperature the HT process has already proceeded for some time, say t_1, with the former rate. This yields a surviving fraction $P_1 < 1$, corresponding to a transfer radius R_1. Keeping in line with the reaction volume model, the further growth of R is assumed to continue as before, only with a new rate. In order to still express this growth on the form of eq 4, the process is treated as if all the transfer has occurred with the new rate. R may then be expressed as

$$R - R_0 = 1/\beta_2 \ln[k_{02}(\tau + t_2)] \quad (9)$$

where t_2 is the time at the new temperature and τ is the time required to reach R_1 (or P_1) with the new rate. This latter time is found from $R_1 - R_0 = 1/\beta_1 \ln(k_{01}t_1) = 1/\beta_2 \ln(k_{02}\tau)$, where the indices 1 and 2 refer to the former and the new temperature, respectively, which gives $\tau = (k_{01}t_1)^{\beta_2/\beta_1}/k_{02}$. In cases where $k_{02} \gg k_{01}$ (and $\beta_2 \leq \beta_1$), τ will be small or negligible compared to t_2.

Figure 5 shows the upper and lower limits of the surviving fraction P at different temperatures for several normal and deuterated doped crystals that have been irradiated at approximately 10 K and annealed at the temperatures indicated. The fractions are relative to the oxidation product concentration at 10 K and have been estimated by assuming equal amounts of oxidation and reduction products throughout the temperature range. Also included in the figure is the fraction of the donors surviving both HT and recombination ($[RC]/[RC]|_{t=0}$). The steep decline of P at the higher temperatures implies a substantial increase in the HT rate and suggests that τ in eq 9 is small and comparable to the experimental error for t_2. This error is connected both to the warming rate and to the thermal conductivity of the crystals and appeared to be of the order of a few minutes. Figure 6 shows the tunneling radii $R - R_0$ for the samples from Figure 5, calculated by eqs 3 and 8 (lower limit for P) and plotted on a logarithmic time scale. For the reasons mentioned above, the starting point on the time axis was set somewhat tentatively at about the middle of the warming period (which was a few minutes). One exception is for the deuterated series at 85 K where the HT rate was too low to assume τ to be negligible (judging by Figures 3 and 5, the rate seems comparable to the rate for normal crystals at 10 K). Instead, τ was estimated by optimizing the fit of the data points to a straight line (eq 9). The rate parameters for all the series were obtained as explained above and are given in Table 1.

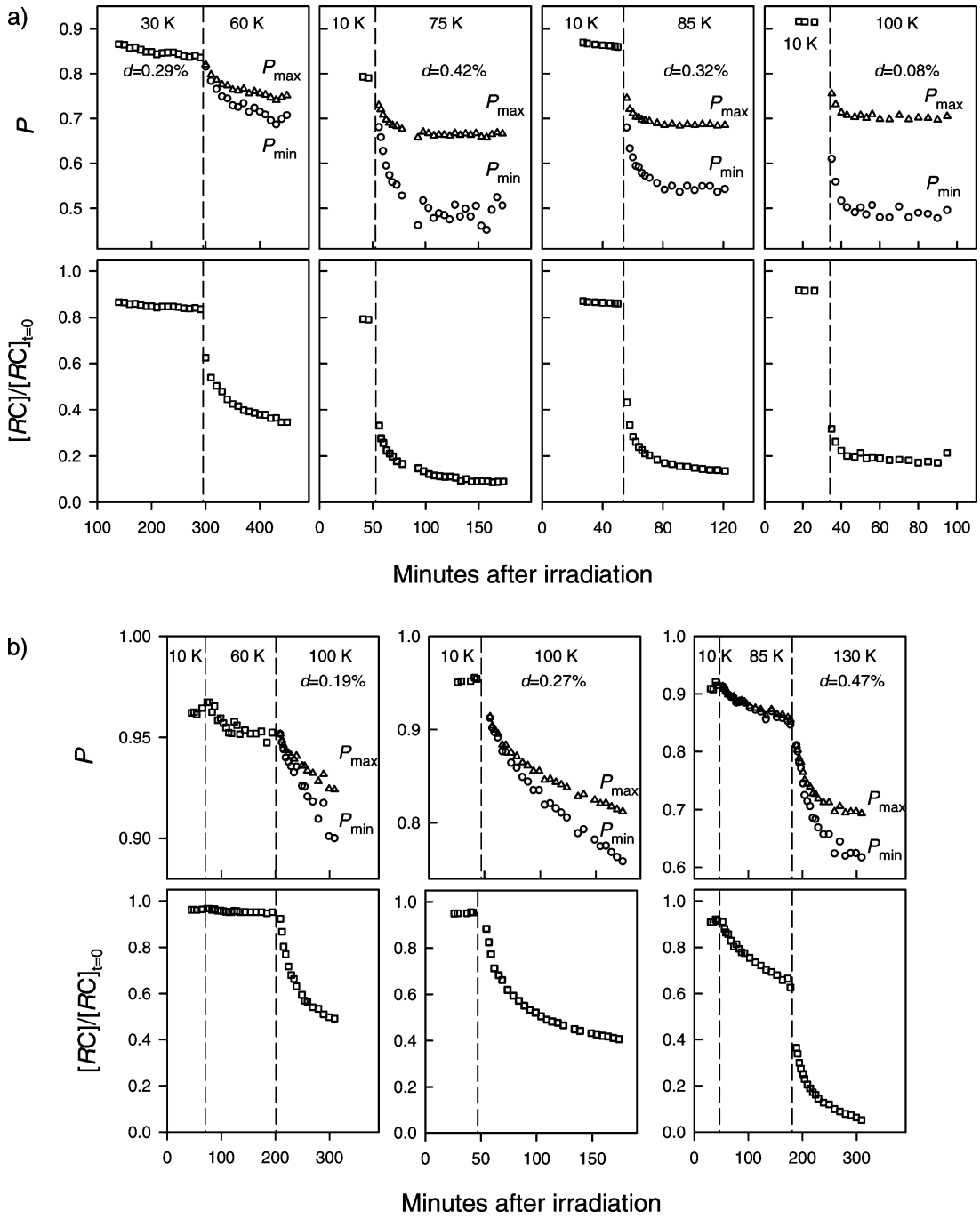

Figure 5. Surviving fraction of donors in absence of recombination (P) and total donor surviving fraction ($[RC]/[RC]_{t=0}$) in (a) normal and (b) deuterated cytosine/thiocytosine crystals, X irradiated at 10 K, and warmed to the temperatures indicated. The fractions are relative to the initial oxidation product concentration at 10 K and have been obtained as explained in the text. The dashed lines mark the start of the warming. The different fractions appear in separate plots to enhance the resolution.

Unfortunately, the procedures above make it difficult to estimate errors with any reasonable confidence. Hence, only the errors resulting from fitting the data to a straight line are given.

The relatively large (orientation-averaged) values for β around 1 Å^{-1} indicate that the HT is mediated by the single-step exchange or superexchange mechanism and that hopping by self-exchange HT, which should give a far lower value,[28] is not activated. Figure 7 shows the rate constants (k_0) in Table 1 in a double logarithmic plot as a function of temperature. For the normal crystals, at 10−40 K the rates are slow and only weakly dependent on temperature. A transition to an Arrhenius-type temperature-dependent rate occurs at around 40−50 K. Judging from Figure 3b, the HT in the deuterated crystals is also activated at around 50−60 K, although the far lower rate makes the transition less pronounced. In the activated region, for the normal crystals, the activation energy $E_a = \mathrm{d}(\ln k_0)/\mathrm{d}(1/k_B T)$ becomes around 0.1−0.2 eV. Below this region, the transfer probability might be dominated by temperature-independent nuclear tunneling through the reaction barrier,[36] which will be discussed in the next section.

The KIE (k_{0H}/k_{0D}) appears to be of the order of 10^6 at 85 and 100 K. This value may seem too large, and some of this huge effect could result from the large uncertainty inherent in the rate parameter values. For instance, the tunneling radius at 100 K (non-deuterated) in Figure 6 may appear overestimated. However, by using the value of k_{0H} at 85 K as a lower limit for the rate at 100 K and the k_{0H} value at 60 K as an upper limit for the 100 K rate for the deuterated crystals (see Figure 6), the

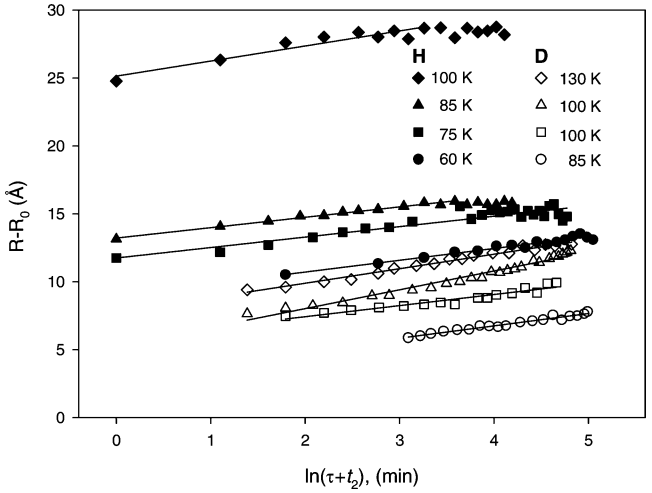

Figure 6. Tunneling distance as a function of ln(time) for HT in single crystals of normal (filled symbols) and deuterated (open symbols) cytosine/thiocytosine. The crystals have been X irradiated at 10 K and warmed to the temperatures indicated. The lines are linear fits to the data. The transfer rate parameters, as well as the doping levels, are given in Table 1 and were obtained as explained in the text. At 85 and 100 K in Figure 5a, *P* rapidly reaches a level after which no further reduction is observed. This could possibly be an effect of inhomogeneous donor distribution.[31,32] For this reason, only the data points until reaching this plateau were used in the straight line fit.

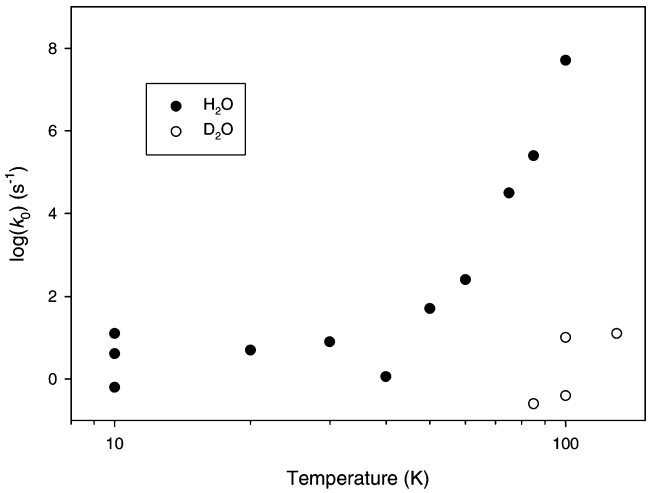

Figure 7. Rate constant ($k_{0)}$ vs temperature for HT (PCHT) in normal (H_2O) and partially deuterated (D_2O) single crystals of cytosine·H_2O doped with thiocytosine.

KIE would still be greater than 10^3. This strongly suggests a proton-coupled hole transfer (PCHT) reaction.[1−4] Scheme 1 shows the possible formation of radical *R*S. HT from radical *R*C to the hole acceptor TC may occur in combination with a re-protonation of *R*C (PT1) and a deprotonation of the oxidized TC (PT2). Whether this reaction is stepwise or concerted is discussed in the next section. While the PT takes place between neighboring bases, the HT may be long-range with several intervening molecules between donor and acceptor.

Equilibrium energies for the reactants and products in Scheme 1 were calculated by DFT as explained above. The calculations were performed on single molecules in the gas phase, and the results serve only as a guide; the surrounding hydrogen-bonded molecules should be included in the calculations to obtain more accurate values. Table 2 shows the equilibrium energy changes (ΔE_0) for the individual and combined steps in Scheme 1. Only HT in combination with PT1 is an exothermic reaction.

SCHEME 1: Formation of the Thiocytosine Deprotonated Cation (Radical RS) by PCHT

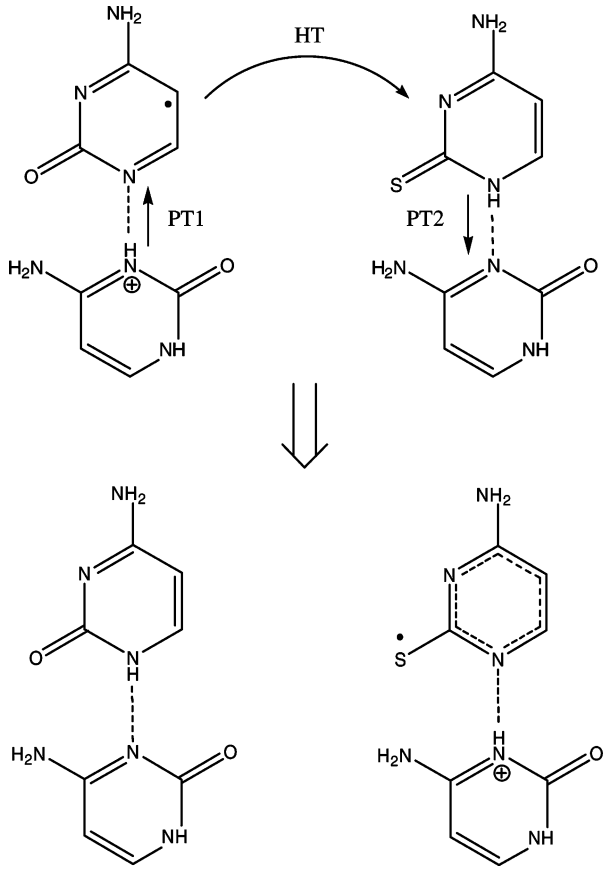

A rough estimation of the (total) reorganization energy λ for the activated PCHT reaction is found from the Marcus relation $E_a = (\Delta G_0 + \lambda)^2/4\lambda$ [37] (for the high-temperature limit) by assuming that the free energy change $\Delta G_0 \approx \Delta E_0 = -(0.62-0.74)$ eV and $E_a = 0.1-0.2$ eV, which gives $\lambda \approx 1.4-2.0$ eV.

3.2. Recombination. No radical decay was observed when warming from 10 to 30 K, whereas at 60 K, the decay had been activated. The decay in the deuterated crystals was activated at about the same temperature as for the normal ones, although with a significantly lower rate. Figure 8 shows the decay of total radical concentration in an undoped normal crystal that has been irradiated at 10 K and subsequently warmed to 60, 100, and 150 K. The decay is plotted as a function of time after irradiation (Figure 8a) and as a function of time after warming on a logarithmic time scale (Figure 8b). The use of separate time scales (Figure 8b), corresponding approximately to time spent at the different temperatures, may be justified by the same arguments as above for the HT and by noticing that the decay rate increases significantly at each temperature. The similar shape of the curves suggests the same decay process at the three temperatures. Most importantly, spectral reconstruction showed that the relative amount of the reduction and oxidation radicals stayed about the same during the whole period, as previously observed,[38] indicating recombination by electron transfer (ET) from *R*A to *R*C. A large part of the ionizations normally occurs through "soft" collisions which may leave the ejected electrons in short enough distances from the parent holes to make the single-step superexchange mechanism efficient.

TABLE 2: Equilibrium Energy Changes Calculated by DFT for the Hole and Proton Transfer in Scheme 1

	HT	PT1	PT2	HTPT1	HTPT2	HTPT1PT2
ΔE_0 (eV)	4.51	0.47	0.13	−0.62	4.39	−0.74

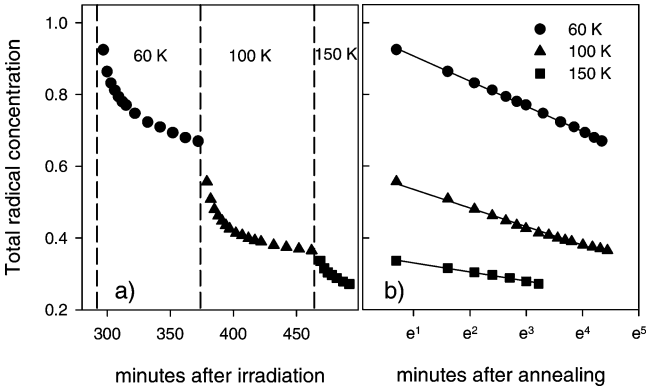

Figure 8. Decay of total radical concentration in a single crystal of undoped cytosine H_2O X irradiated at 10 K and annealed to the temperatures indicated plotted as (a) a function of time after irradiation and (b) on a logarithmic time scale as a function of time after annealing. The concentration is relative to the total radical yield at 10 K. The dashed lines mark the beginning of the annealing and the solid lines are linear fits to the data. The average r^2 factors were 0.991, 0.991, and 0.985 for the spectrum reconstruction at 60, 100, and 150 K, respectively.

The plots in Figure 8b are approximately linear, which is a typical trait when having a dispersion of distances between the reactants.[39] By treating the recombining radicals as isolated donor−acceptor pairs, the surviving fraction $n(t)$ of these pairs may be expressed as $n(t) = \int_0^\infty \exp[-k(r)t]f(r)\,dr$ where $f(r)$ is the (normalized) distribution of the pairs with respect to their separation r. In the simple case of a rectangular distribution of pair separations, it can be shown that $n(t)$ eventually will decrease proportionally to $(1/\beta)\ln(k_0t)$,[39] in agreement with the linearity in the plots. To obtain a rough estimate of the temperature effect on the ET rate, the decay rates may be compared for two temperatures at the same radical concentration. Extrapolating the 60 K curve in Figure 8b, using either the slope of the 60 or that of the 100 K curve, to the first experimental value at 100 K gives that $k_{100K}/k_{60K} \sim 10^2-10^3$. The same procedure gives that $k_{150K}/k_{100K} \sim 10^2$. This suggests an Arrhenius-type temperature dependence (and possibly a lower activation energy for the recombination than for the hole shift).

Figure 9 shows the decay of total radical concentration for some of the crystals in Figure 5 and two undoped normal crystals (one being the crystal from Figure 8). The crystals were all irradiated at approximately 10 K and warmed to the temperatures indicated. The decay rates for deuterated crystals at 100 K and for normal crystals at 60 K are similar and, based on the discussion above, suggest a KIE $> 10^2$ at 100 K. At higher temperatures (140−150 K), no significant KIE is observed. While radical *R*S in normal crystals was stable at 100 K, warming to 150 K resulted in these radicals also decaying linearly on a logarithmic time scale (data not shown), which indicates a higher activation energy for the recombination of this radical species. In the deuterated crystals, radical *R*S started to decay between 140 and 170 K. The KIE could not easily be estimated but appeared to be large (as can be seen in Figure 3).

The electron- and proton-transfer reactions that may be involved in the recombination are depicted in Scheme 2. Table 3 shows the equilibrium energy changes calculated by DFT for the reactions in Scheme 2. The calculations were also performed for recombination of radical *R*S with radical *R*A. The ET must be accompanied with the transfer of a proton for the reaction to be exothermic, which, together with the large KIE at low temperatures, suggests that the reaction is PCET.

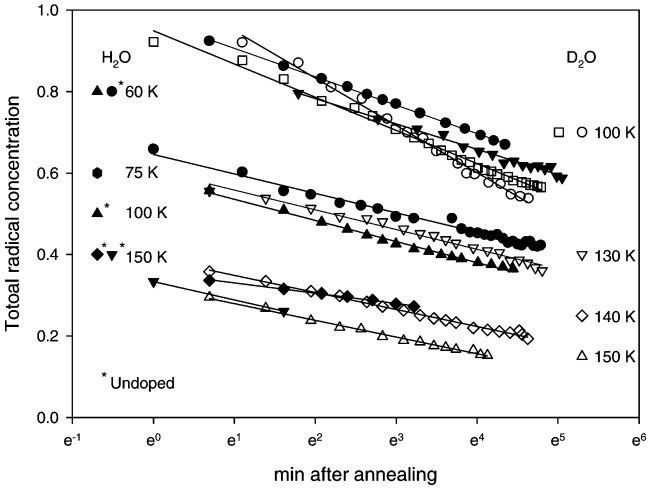

Figure 9. Decay of total radical concentration in normal and deuterated single crystals of cytosine·H_2O (D_2O) doped with thiocytosine (doping level 0−0.5 mol %) irradiated at 10 K and annealed to the temperatures indicated. The concentration is relative to the total radical yield at 10 K. The decay is plotted on a logarithmic time scale as a function of time after annealing. The fully drawn lines are linear fits to the data.

SCHEME 2: Recombination of Radicals RC and RA

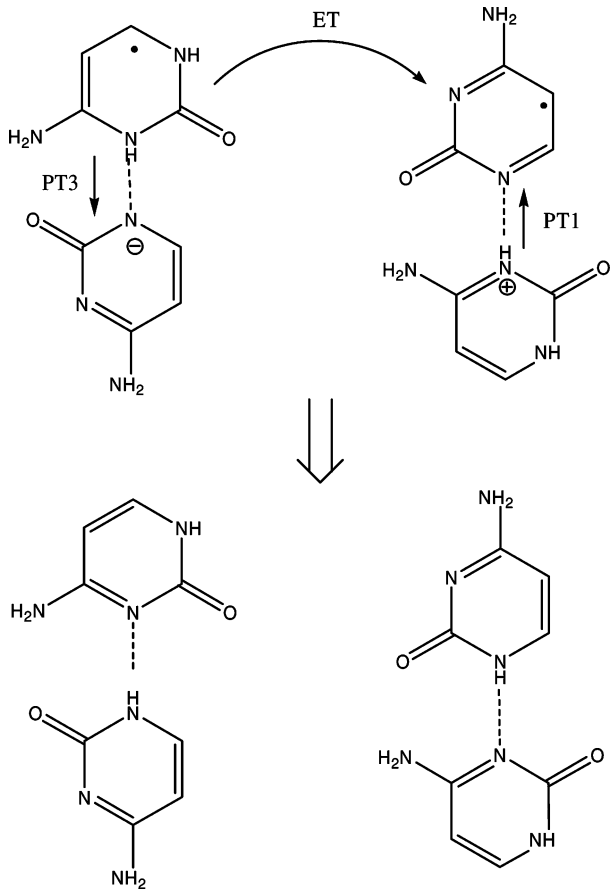

4. Discussion

The huge KIE of apparently $>10^3$ for the hole shift (and $>10^2$ for the recombination) strongly indicates a coupling with proton transfer. This PCHT reaction can be stepwise or concerted. The huge KIE and the large endothermicity of several eV for single HT indicate that if the transfer is stepwise then proton transfer (PT1) must precede the hole transfer step (PT1/HT).[40] A concerted transfer (HPT1) will have a smaller effective coupling between reactant and product state than the single PT step,

TABLE 3: Equilibrium Energy Changes Calculated by DFT for the Recombination PCET Reactions Shown in Scheme 2

	ET	PT1	PT3	ETPT1	ETPT3	ETPT1PT3
$\Delta E_0{}^a$ (eV)	2.30	0.47	0.22	−2.83	−2.83	−7.96
$\Delta E_0{}^b$ (eV)	2.74	0.13	0.22	−2.08	−2.39	−7.21

[a] Recombination of *R*C and *R*A. [b] Recombination of *R*S and *R*A.

because of the combined tunneling events of both the hole and the proton, while the reaction barrier is likely to be smaller as the reaction is highly exothermic.[3] There is then a competition between a lower barrier for HPT1 and a larger coupling for PT1/HT. Some aspects point to a concerted transfer. First, according to the DFT calculations, PT1 in isolation is not thermodynamically favorable, and ENDOR studies of this and similar systems have not revealed the presence of a pristine oxidized cation radical.[20] This suggests that back-transfer of the protons for radical *R*C is highly unlikely at low temperatures. The stable EPR signals of undoped crystals in the present work at 10 K also support that suggestion. Second, the low temperatures involved suggest that the reaction channel with the lower barrier will dominate, in agreement with the estimated activation energy of 0.1−0.2 eV for the hole shift reaction being lower than the estimate of ΔE_0 for PT1 (0.47 eV). Third, if the reaction is stepwise, then the large barrier for PT1 together with the large KIE indicate that PT1 would be a rate-limiting step. This should especially be the case for small hole donor−acceptor distances, where the electronic coupling is large and definitely for the deuterated crystals. The overall reaction should then follow first-order kinetics. This would also apply to the decay curves of the recombining radicals. However, none of the curves in Figures 2, 3, 5, 8, or 9 becomes linear in a first-order rate plot. Instead, the curves tend to be linear on a logarithmic time scale, consistent with an exponentially decreasing electronic coupling (and tunneling probability) with distance that would limit the rate for a concerted transfer in this system.[41] Finally, if initial PT should gate the charge transfer,[14] then the apparently lower barrier for PT2 than for PT1 suggests that the decay of radical *R*S should be activated at lower temperatures than those for radical *R*C. It is thus proposed that a concerted transfer is the dominant reaction pathway for charge transfer in this system.

The huge KIE is most likely a result of a large barrier for PT owing to the large proton donor−acceptor equilibrium distance (2.95 Å[23]) and to the PT probably occurring between proton/deuteron vibrational ground states at low temperatures. This would make the coupling, or tunneling probability, for D^+ significantly smaller than that for H^+.[3,42−45] One can also not rule out the possibility of a concerted electron/hole- and double PT (see Schemes 1 and 2) being responsible for the colossal KIE. The reduction in KIE observed for the recombination at higher temperatures may result from increased contribution of reaction channels involving excited proton/deuteron vibrational product states and/or excitation of N1···N3 H-bond stretching modes, both of which are relatively more beneficial for deuteron transfer than for proton transfer.[42]

The activation of the PCHT rate (Figure 7) at around 40−50 K suggests that excitation of low-frequency intermolecular modes activates the transfer. Below this temperature the vibrational modes that couple to the PCHT process may not be thermally excited and the rate might be dominated by temperature-independent nuclear tunneling through the reaction barrier.[36] An expression relating the average effectively coupled mode frequency (ω) for electron transfer to the transition temperature between nuclear tunneling and activated rate, $k_BT \approx \hbar\omega/4$,[46] gives for $T = 40-50$ K a mode frequency in the region $\hbar\omega \approx 110-140$ cm^{-1}. Several intense Raman active low-frequency modes in crystals of cytosine monohydrate have been observed in the region 54−137 cm^{-1}.[47,48]

Another possibility would be two (or more) different reaction channels; one activated process and one slow, approximately activationless or barrierless process for which the potential energy surfaces for reactants and products cross at the minimum of the reactant state.[49] However, given that the reactants are the same and since the hole donor−acceptor distances are unlikely to differ for two such reactions, it is difficult to envisage a substantially lower rate for an activationless process. The low rate below 50 K may instead indicate a nuclear tunneling phenomenon.

The thermal activation of both the hole shift and the recombination of *R*C and *R*A in the same narrow temperature range may suggest that both reactions are coupled to the same vibrational modes. These modes (assumedly below 140 cm^{-1}) likely involve translational and librational motion of the cytosine molecules.[48] Thus, apart from equalizing the energy levels of reactants and products, excitation of these modes may reduce the PT barrier and increase the overall PCHT/PCET coupling by causing contraction in the N1···N3 hydrogen bond, thereby activating other kinetically more favorable reaction channels.[50] The presumable conversion of radical *R*A which is activated at around the same temperature (see Experimental Section) may also be connected to this effect.

In relation to radical reactions in DNA, it can be expected that radicals stabilized by PT between the cytosine−guanine base-pairs are prone to charge shift and recombination even at very low temperatures through a concerted transfer and coupling with low-frequency H-bond modes.[51−53] Radical recombination in DNA takes place at very low temperatures with decay characteristics similar to those in Figures 5, 8, and 9,[8,14,15,54] which suggests that the annealing behavior in DNA may be due to a dispersion of distances, and thus electronic coupling strengths, between the reactants rather than a dispersion in activation energies which has previously been proposed.[8,14] The present findings also have some resemblances to other low-temperature EPR studies of excess single ET to an intercalator in irradiated DNA that revealed a temperature-independent rate between 4 and 77 K with a β value around 1 Å^{-1}.[15] In contrast however, the reported[55] high rate constant (k_0) of the order of 10^{11} s^{-1} may indicate that the temperature-independence is due to the reaction being activationless instead of a nuclear tunneling process through a barrier.

5. Conclusions

The main results are the following: First, a huge KIE for the hole shift from radical *R*C to *T*C and for the recombination of radicals *R*C and *R*A (> 10^2-10^3 at 100 K) indicates a proton-coupled electron/hole transfer reaction. Second, the kinetic curves obtained, together with DFT calculations, indicate that this reaction is concerted. Third, the distance decay constant β for the hole transfer was estimated to be around 1 Å^{-1} throughout the temperature range studied (10−100 K), indicating a superexchange mechanism as opposed to hopping. Fourth, both the PCHT and the recombination (PCET) become activated at around 40−50 K and seem to exhibit an Arrhenius-type temperature-dependence. Below the transition temperature, the PCHT rate is slow ($k_0 \sim 10^0-10^1$ s^{-1}) and only weakly temperature dependent, which may indicate a transition from nuclear tunneling to activated rate by thermal excitation of the low-frequency vibrational modes that couple to the PCHT/PCET processes.

Acknowledgment. We thank Dr. Eirik Malinen who participated in the early stages of this work, Mr. Efim Brondz for his technical assistance, and Mr. Dirk Petersen for recording the NMR spectra. The work is partly supported by the Croatian Ministry of Science, Education and Sports (Grant 006-006117-1237). J.N.H. acknowledges the Royal Chemical Society Journals Grant Award for supporting the visit to the University of Oslo. Some of the crystals studied were kindly supplied by Dr. K. Sanković.

References and Notes

(1) Cukier, R. I. *J. Phys. Chem.* **1994**, *98*, 2377.
(2) Cukier, R. I.; Nocera, D. G. *Annu. Rev. Phys. Chem.* **1998**, *49*, 337.
(3) Decornez, H.; Hammes-Schiffer, S. *J. Phys. Chem. A* **2000**, *104*, 9370.
(4) Soudackov, A.; Hammes-Schiffer, S. *J. Chem. Phys.* **2000**, *113*, 2385.
(5) Nelson, W. H.; Sagstuen, E.; Hole, E. O.; Close, D. M. *Radiat. Res.* **1992**, *131*, 10.
(6) Bernhard, W. A.; Barnes, J.; Mercer, K. R.; Mroczka, N. *Radiat. Res.* **1994**, *140*, 199.
(7) Nelson, W. H.; Sagstuen, E.; Hole, E. O.; Close, D. M. *Radiat. Res.* **1998**, *149*, 75.
(8) Bernhard, W. A.; Close, D. M. DNA Damage Dictates the Biological Consequences of Ionizing Irradiation: The Chemical Pathways. In *Charged Particle and Photon Interactions with Matter*; Mozumber, A., Hatano, Y., Eds.; Marcel Dekker: New York, 2003; pp 431.
(9) Steenken, S. *Free Rad. Res. Commun.* **1992**, *16*, 349.
(10) Steenken, S. *Biol. Chem.* **1997**, *378*, 1293.
(11) Weatherly, S. C.; Yang, I. V.; Thorp, H. H. *J. Am. Chem. Soc.* **2001**, *123*, 1236.
(12) Shafirovich, V.; Dourandin, A.; Geacintov, N. E. *J. Phys. Chem. B* **2001**, *105*, 8431.
(13) Giese, B.; Wessely, S. *Chem. Commun.* **2001**, 2108.
(14) Debije, M. G.; Bernhard, W. A. *J. Phys. Chem. B* **2000**, *104*, 7845.
(15) Cai, Z. L.; Gu, Z. Y.; Sevilla, M. D. *J. Phys. Chem. B* **2000**, *104*, 10406.
(16) Close, D. M. *J. Phys. Chem. B* **2003**, *107*, 864.
(17) Sanković, K.; Krilov, D.; Herak, J. N. *Radiat. Res.* **1991**, *128*, 119.
(18) Herak, J. N.; Sanković, K.; Hole, E. O.; Sagstuen, E. *Phys. Chem. Chem. Phys.* **2000**, *2*, 4971.
(19) Sanković, K.; Malinen, E.; Medunić, Z.; Sagstuen, E.; Herak, J. N. *Phys. Chem. Chem. Phys.* **2003**, *5*, 1665.
(20) Sagstuen, E.; Hole, E. O.; Nelson, W. H.; Close, D. *J. Phys. Chem.* **1992**, *96*, 8269.
(21) Krivokapić, A.; Hole, E. O.; Sagstuen, E. *Radiat. Res.* **2003**, *160*, 340.
(22) Jeffrey, G.; Kinoshita, Y. *Acta Crystallogr.* **1963**, *16*, 20.
(23) Weber, H. P.; Craven, B. M.; McMullan, R. K. *Acta Crystallogr.* **1980**, *B36*, 645.
(24) Frisch, M. J. T., G. W.; Schlegel, H. B.; Scuseria, G. E.; Robb, M. A.; Cheeseman, J. R.; Montgomery, Jr., J. A.; Vreven, T.; Kudin, K. N.; Burant, J. C.; Millam, J. M.; Iyengar, S. S.; Tomasi, J.; Barone, V.; Mennucci, B.; Cossi, M.; Scalmani, G.; Rega, N.; Petersson, G. A.; Nakatsuji, H.; Hada, M.; Ehara, M.; Toyota, K.; Fukuda, R.; Hasegawa, J.; Ishida, M.; Nakajima, T.; Honda, Y.; Kitao, O.; Nakai, H.; Klene, M.; Li, X.; Knox, J. E.; Hratchian, H. P.; Cross, J. B.; Bakken, V.; Adamo, C.; Jaramillo, J.; Gomperts, R.; Stratmann, R. E.; Yazyev, O.; Austin, A. J.; Cammi, R.; Pomelli, C.; Ochterski, J. W.; Ayala, P. Y.; Morokuma, K.; Voth, G. A.; Salvador, P.; Dannenberg, J. J.; Zakrzewski, V. G.; Dapprich, S.; Daniels, A. D.; Strain, M. C.; Farkas, O.; Malick, D. K.; Rabuck, A. D.; Raghavachari, K.; Foresman, J. B.; Ortiz, J. V.; Cui, Q.; Baboul, A. G.; Clifford, S.; Cioslowski, J.; Stefanov, B. B.; Liu, G.; Liashenko, A.; Piskorz, P.; Komaromi, I.; Martin, R. L.; Fox, D. J.; Keith, T.; Al-Laham, M. A.; Peng, C. Y.; Nanayakkara, A.; Challacombe, M.; Gill, P. M. W.; Johnson, B.; Chen, W.; Wong, M. W.; Gonzalez, C.; Pople, J. A. *Gaussian 03*, Revision B.03; Gaussian, Inc.: Pittsburgh, PA, 2003.
(25) Sanković, K.; Herak, J. N.; Krilov, D. *J. Mol. Struct.* **1988**, *190*, 277.
(26) Sagstuen, E.; Hole, E. O.; Haugedal, S. R.; Lund, A.; Eid, O. I.; Erickson, R. *Nukleonika* **1997**, *42*, 353.
(27) Sagstuen, E.; Lund, A.; Itagaki, Y.; Maruani, J. *J. Phys. Chem. A* **2000**, *104*, 6362.
(28) Bixon, M.; Jortner, J. *Adv. Chem. Phys.* **1999**, *106*, 35.
(29) Huddleston, R. K.; Miller, J. R. *J. Phys. Chem.* **1982**, *86*, 200.
(30) Miller, J. R.; Beitz, J. V.; Huddleston, R. K. *J. Am. Chem. Soc.* **1984**, *106*, 5057.
(31) The majority of the holes (the donors) induced by the radiation are formed in clusters. This influences the distance distribution between donors and acceptors and thus affects the probability for transfer. The degree of clustering is unknown, and since the issues of interest here are the relative effects of temperature and deuterium substitution (KIE), a random distribution of donors and acceptors will be assumed.
(32) Mozumder, A.; Magee, J. L. *Radiat. Res.* **1966**, *28*, 203.
(33) Miller, J. R.; Beitz, J. V. *J. Chem. Phys.* **1981**, *74*, 6746.
(34) When using this last expression, it has previously been found that k_0 will be too large by a factor 1.9 (see ref 29). When numerical values are quoted, this correction has been made.
(35) Radical *R*S was thermally more stable than *R*C and *R*A at higher temperatures ($\geq$60 K) and a higher stability of radical *R*S during irradiation would result in lower k_0 values than those reported.
(36) Jortner, J. *J. Chem. Phys.* **1976**, *64*, 4860.
(37) Marcus, R. A.; Sutin, N. *Biochim. Biophys. Acta* **1985**, *811*, 265.
(38) Dulčić, A.; Herak, J. N. *Radiat. Res.* **1977**, *71*, 75.
(39) Zamaraev, K. I.; Khairutdinov, R. F. *Russ. Chem. Rev.* **1978**, *47*, 518.
(40) The EPR signal of radical *R*S will be similar and well-separated from the spectral bulk whether deprotonated or not. Thus, PT2 as a subsequent step will not contribute to the KIE.
(41) The possibility of a stepwise reaction for the normal crystals, with HT being rate-limiting, and a concerted transfer for the deuterated crystals is not considered likely as the larger coupling for PT1/HT would be more likely to override the lower barrier for HPT1 for systems with deuterium than for systems with hydrogen.
(42) Kiefer, P. M.; Hynes, J. T. *J. Phys. Chem. A* **2004**, *108*, 11793.
(43) Kiefer, P. M.; Hynes, J. T. *J. Phys. Chem. A* **2004**, *108*, 11809.
(44) Differences in zero point energies for the N−H and N−D bonds, or different p*K* values, assumedly do not contribute significantly to the KIE (see ref 45).
(45) Krishtalik, L. I. *Biochim. Biophys. Acta* **2000**, *1458*, 6.
(46) Buhks, E.; Jortner, J. *J. Phys. Chem.* **1980**, *84*, 3370.
(47) Kugel, G. E.; Gerbaux, X.; Carabatos, C.; Martel, P.; Powell, B. M. *Spectrochim. Acta A* **1979**, *35*, 1155.
(48) Weber, I.; Kirin, D. *J. Mol. Struct.* **1992**, *267*, 67.
(49) Jortner, J. *J. Am. Chem. Soc.* **1980**, *102*, 6676.
(50) Since the electrons/holes and the protons generally transfer in different directions the excitation of these modes may not be expected to enhance the electronic coupling between electron/hole donor and acceptor.
(51) Li, X. F.; Cai, Z. L.; Sevilla, M. D. *J. Phys. Chem. B* **2001**, *105*, 10115.
(52) Kabanov, A. V.; Komarov, V. M.; Yakushevich, L. V.; Teplukhin, A. V. *Int. J. Quantum Chem.* **2004**, *100*, 595.
(53) Brauer, B.; Gerber, R. B.; Kabelac, M.; Hobza, P.; Bakker, J. M.; Riziq, A. G. A.; de Vries, M. S. *J. Phys. Chem. A* **2005**, *109*, 6974.
(54) Pal, C.; Hüttermann, J. *J. Phys. Chem. B* **2006**, *110*, 14976.
(55) Messer, A.; Carpenter, K.; Forzley, K.; Buchanan, J.; Yang, S.; Razskazovskii, Y.; Cai, Z.; Sevilla, M. D. *J. Phys. Chem. B* **2000**, *104*, 1128.